Cell

Gene Expression Is Circular: Factors for mRNA Degradation Also Foster mRNA Synthesis

Gal Haimovich,[1,6] Daniel A. Medina,[2] Sebastien Z. Causse,[3] Manuel Garber,[4] Gonzalo Millán-Zambrano,[5] Oren Barkai,[1] Sebastián Chávez,[5] José E. Pérez-Ortín,[2] Xavier Darzacq,[3] and Mordechai Choder[1,*]

[1]Department of Molecular Microbiology, Rappaport Faculty of Medicine, Technion-Israel Institute of Technology, Haifa 31096, Israel
[2]Departamento de Bioquímica y Biología Molecular, Facultad de Biológicas and ERI Biotecmed, Universitat de València, Dr Moliner 50, E-46100 Burjassot, Valencia, Spain
[3]Functional Imaging of Transcription, CNRS UMR 8197, IBENS, Institute of Biology, École Normale Supérieure, 46 rue d'Ulm, 75005 Paris, France
[4]University of Massachusetts Medical School, 55 Lake Avenue North, Worcester, MA 01655 USA
[5]Departamento de Genética, Facultad de Biología, Universidad de Sevilla, Avenida Reina Mercedes 6, E-41012 Sevilla, Spain
[6]Current address: Anatomy and Structural Biology, Albert Einstein College of Medicine, 1300 Morris Park Avenue, Bronx, NY 10461, USA
*Correspondence: choder@technion.ac.il
http://dx.doi.org/10.1016/j.cell.2013.05.012

SUMMARY

Maintaining proper mRNA levels is a key aspect in the regulation of gene expression. The balance between mRNA synthesis and decay determines these levels. We demonstrate that most yeast mRNAs are degraded by the cytoplasmic 5′-to-3′ pathway (the "decaysome"), as proposed previously. Unexpectedly, the level of these mRNAs is highly robust to perturbations in this major pathway because defects in various decaysome components lead to transcription downregulation. Moreover, these components shuttle between the cytoplasm and the nucleus, in a manner dependent on proper mRNA degradation. In the nucleus, they associate with chromatin—preferentially ~30 bp upstream of transcription start-sites—and directly stimulate transcription initiation and elongation. The nuclear role of the decaysome in transcription is linked to its cytoplasmic role in mRNA decay; linkage, in turn, seems to depend on proper shuttling of its components. The gene expression process is therefore circular, whereby the hitherto first and last stages are interconnected.

INTRODUCTION

Gene expression is traditionally divided into several stages, including mRNA synthesis and processing, export (in eukaryotes), translation, and decay. Yet, gene expression can be viewed as a single system in which all stages are mechanistically coupled (Komili and Silver, 2008) and coordinated by master regulators (Harel-Sharvit et al., 2010). An essential and well-controlled component of this system is the cytoplasmic mRNA decay pathway, considered to represent the endpoint of the mRNA life. Following shortening of the mRNA poly(A) tail by the Ccr4/Not and Pan2/3 complexes, the eukaryotic mRNA can then be degraded by two pathways: from 3′ to 5′ by the exosome or from 5′ to 3′ by the Xrn1p exonuclease (Garneau et al., 2007; Parker, 2012; Pérez-Ortín et al., 2013; Haimovich et al., 2013). The latter pathway involves prior removal of the 5′-cap by the Dcp2p enzyme, assisted and regulated by Dcp1p, Pat1p, Dhh1p, Edc1/2/3p, and the Lsm1-7 complex. Conventional wisdom holds that, following the completion of the degradation of a certain mRNA, the mRNA decay factors (DFs) re-enter the decay process of yet another mRNA in the cytoplasm. Other options have not been systematically examined.

Here, we report that all tested DFs shuttle between the cytoplasm and the nucleus, associate preferentially with transcription start-sites and stimulate transcription initiation and elongation. Moreover, import of DFs depends on the capacity of Xrn1p to function in mRNA degradation. Various statistical analyses uncovered a linkage between the functions of Xrn1p in mRNA synthesis and decay. We propose that the synthetic and decay processes represent two arms of a larger machinery, the "synthegradosome."

RESULTS

Steady State mRNA Levels Are Highly Robust to Perturbations in mRNA Decay

The rates of mRNA synthesis and decay determine the steady-state level of mRNA (also referred herein as m*R*NA *a*bundance [RA]). Accordingly, a defect in mRNA decay is expected to result in an increase in mRNA levels. As expected, elevated levels of *EDC1* and *RPS28B* mRNAs were observed in cells lacking various genes encoding DFs (Figure 1A and Figure S1A available online) (Badis et al., 2004; Muhlrad and Parker, 2005). Surprisingly, the levels of various other mRNAs did not increase in strains lacking these DFs (Figures 1A and S1A) and some levels even decreased, despite their increased stabilities (Figure 1B). These

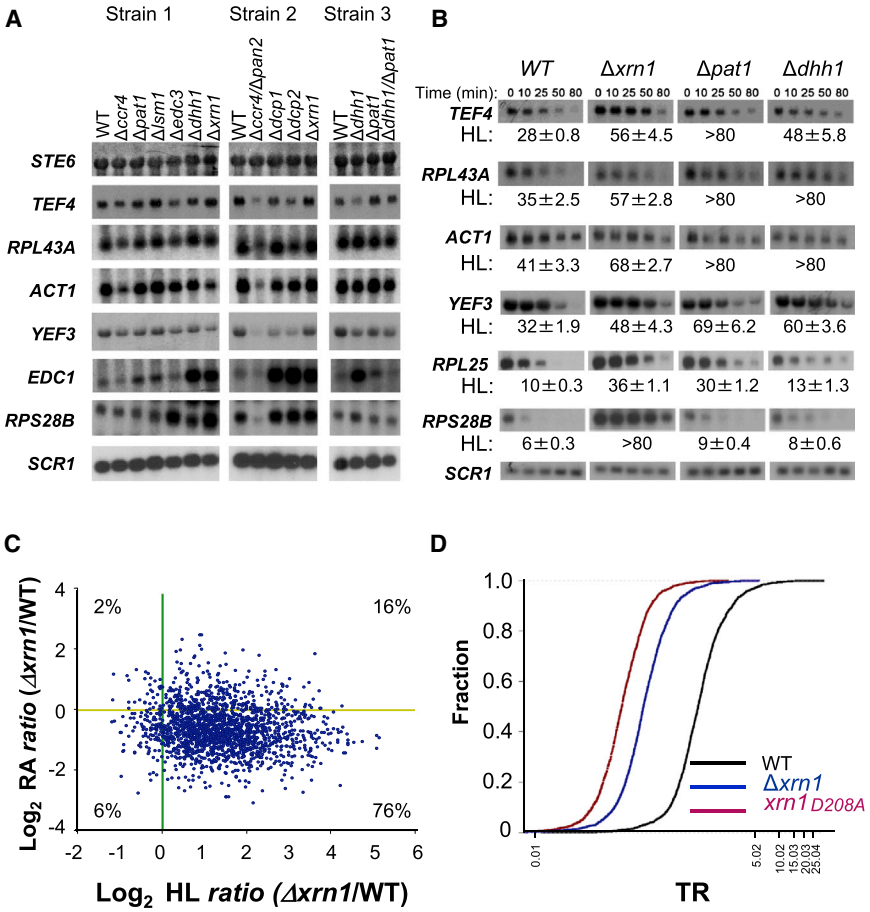

Figure 1. Transcription of Most Genes Is Downregulated in Strains Defective in 5′-3′ mRNA Decay

(A) Deletions of various mRNA decay factors do not lead to mRNA accumulation. Northern blot hybridization images of mRNAs from the indicated deletion strains (genetic backgrounds: strain 1, yMC229; strain 2, yMC370; strain 3, yMC375). The same membrane was probed with the indicated probes. Quantification of the signals in (A) is presented in Figure S1A. *SCR1* RNA (Pol III transcript) was used for normalization.

(B) Decay of the indicated mRNAs at 30°C was determined after blocking transcription by 1, 10-phenanthroline. Half life (HL) ± SD is indicated below each autoradiogram.

(C) Scatter plot data from thiolutin shutoff assay (Pelechano and Pérez-Ortín 2008) showing Log_2 ratios (Δ*xrn1*/WT) of HL versus the ratio (Δ*xrn1*/WT) of mRNA steady-state level—determined before adding the drug (RA). Spots below the horizontal line and on the right side of the vertical line represent mRNAs whose RA decreased and stability increased. The percentage of genes in each quadrant is indicated; n = 1811 genes.

(D) Cumulative distribution of transcriptional rates (TR) in arbitrary units.

See also Figure S1 and Tables S1, S2, and S4.

results prompted us to obtain a whole-genome view of both the half-lives (HL) and RAs (Pelechano and Pérez-Ortín 2008). First, we found that Xrn1p—the only known cytoplasmic 5′ to 3′ exonuclease—is involved in the degradation of most, if not all, mRNAs (Figures 1C and S1C, and Table S1). Thus, as proposed previously (Anderson and Parker, 1998; Coller and Parker, 2004; Parker, 2012), Xrn1p-mediated decay is a major cytoplasmic pathway for mRNA degradation in yeast. Second, consistent with the northern analysis, most spots scattered around or below the ratio 1. Importantly, no correlation was found between the effect of *XRN1* deletion on HLs and its effect on RA (Figure 1C). Table S1 shows a list of mRNAs whose stability was severely affected by *XRN1* deletion, but their RA was little perturbed. These observations suggest that changes of HL are compensated by inverse changes in mRNA synthesis, as was observed in a number of specific cases (Table S2, see also legend). These results are consistent with previous data demonstrating that the levels of most mRNAs in Δ*xrn1* and Δ*dcp1* cells are not higher than those in wild-type (WT) cells (He et al., 2003; Muhlrad and Parker, 1999). We therefore hypothesized that, in addition to their role in mRNA decay, the DFs have the capacity to enhance transcription, either directly or indirectly. This notion is supported by prior studies demonstrating numerous physical and genetic interactions of various DFs with factors that are involved in the nuclear stages of gene expression (Table S3 and Figure S1B).

Disruption of Xrn1p Compromises Transcription of Most Genes

To obtain a whole-genome view of transcription rates (TRs), we performed genomic run-on (GRO) experiments (García-Martínez et al., 2004; Pelechano and Pérez-Ortin, 2010). We found that TRs of most genes were downregulated in Δ*xrn1* cells ($p < 10^{-15}$, KS test, median of 4.6-fold, Figure 1D, *Δxrn1*).

$Xrn1^{D208A}p$ is an inactive form of the enzyme that is expressed at WT level and binds uncapped mRNA as efficiently as Xrn1p but does not degrade it (Solinger et al., 1999). Proliferation rate of $xrn1^{D208A}$ and Δ*xrn1* strains are comparable (Figure S1E; Solinger et al., 1999), and they exhibit similar levels of P bodies (Figure S1F). More importantly, cumulative distribution of HLs in the two mutants is comparable (Figure S1C). Nevertheless, $xrn1^{D208A}$ cells were more defective than the Δ*xrn1* cells in transcription (Figures 1D and S1D) (median of 8.5-fold, $p < 10^{-15}$ KS test). TR values are listed in Table S4.

Transcriptional Induction Is Dependent on mRNA Decay Factors

Next, we investigated de novo mRNA synthesis and mRNA decay in response to various environmental signals. As expected (Lohr et al., 1995), galactose stimulation rapidly induced transcription of *GAL* genes in WT cells (Figure 2A), and glucose addition led to rapid transcriptional repression (Lohr et al., 1995), followed by mRNA degradation (Figure 2B). Accumulation of mRNA in the $xrn1^{D208A}$ strain lagged behind

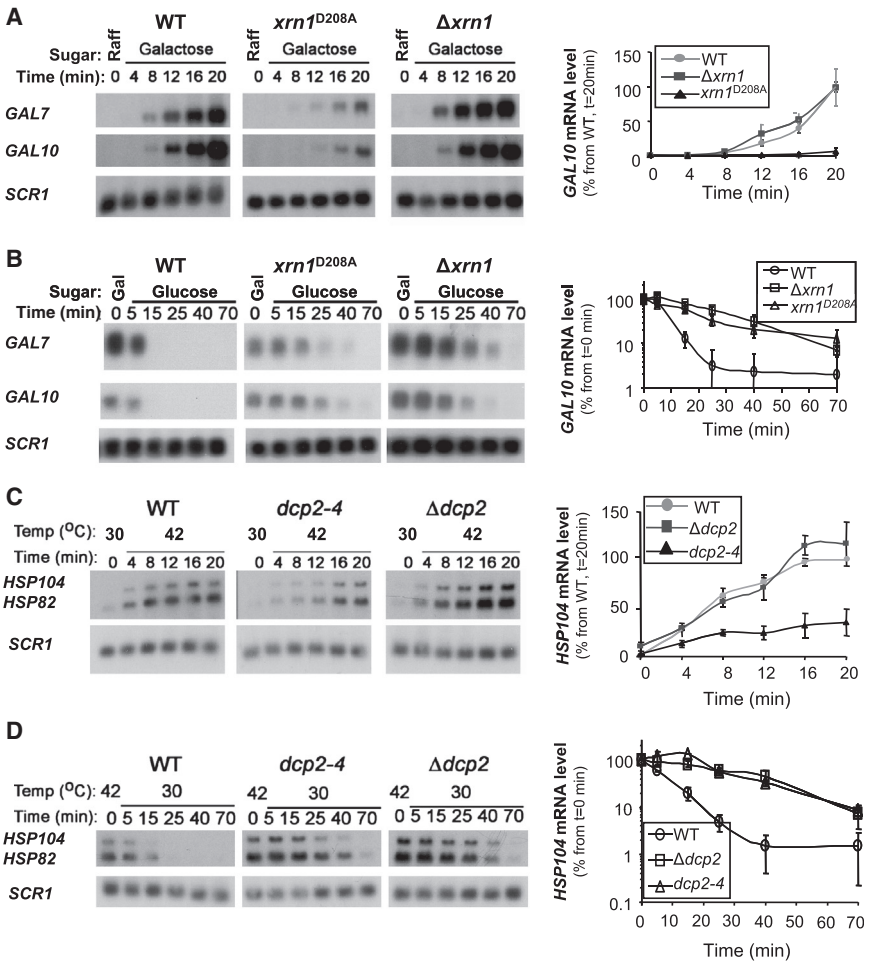

Figure 2. Transcriptional Induction by Various Inducers Is Dependent on Enzymatically Active Xrn1p and Dcp2p

(A and B) Transcriptional induction of *GAL* genes (A) and decay of *GAL* mRNAs (B) was performed on the indicated strains as described in Experimental Procedures. Shown are northern blot images (left) and quantification (right), performed as in Figure S1 except that results are shown as percentage relative to time point 20 min of WT (in A) or 0 min of each strain (in B).

(C) Northern analysis showing induction of the indicated HS genes by temperature shift up. Quantification was performed as in Figure 2A.

(D) To examine mRNA decay, transcription of the indicated HS genes was inhibited by shifting the temperature down, and the levels of the indicated mRNAs were monitored by northern analysis and quantified as in Figure 2B. *SCR1* RNA is shown for loading control and was used for normalization. Error bars in all panels represent SD of three assays. See also Figure S2.

the WT, indicating a clear defect in transcriptional induction (Figure 2A). Although deletion of *XRN1* led to stabilization of *GAL* mRNAs (Figure 2B), mRNA accumulation in the Δ*xrn1* strain was comparable to that in the WT cells (Figure 2A), suggesting a defect in transcription in this mutant as well—consistent with the GRO results. Significantly, because the effect of D208A mutation on mRNA stability was identical to that of *XRN1* deletion (Figure 2B), we concluded that the different accumulation of mRNAs in these mutants (shown in Figure 2A) is solely due to a difference in their transcriptional capacity.

We also assessed transcriptional induction and mRNA decay of heat shock (HS) genes in response to HS, and non-HS genes during recovery from HS. We compared WT to *xrn1* mutant strains, discussed above. We also examined Δ*dcp2* and *dcp2-4*, encoding enzyme-dead Dcp2^{E153Q}p (Dunckley and Parker, 1999). As shown in Figures 2C, S2A, S2C, and S2E, transcription of these genes was relatively defective in the *xrn1* and *dcp2* mutant strains. The transcriptional defect was, again, more pronounced in both enzyme-dead strains compared to their respective deletion strains, despite comparable stability of their mRNAs (Figures 2B, 2D, S2B, S2D, and S2F).

Interestingly, both transcription and decay of a noncoding RNA were found to be dependent on DFs (Figures S2G–S2I), like those of mRNAs.

Xrn1p Affects Pol II Occupancy on TEF4 Gene

Fluorescent in situ hybridization (FISH) analysis, designed to detect single *TEF4* mRNA molecules and to identify specific nuclear transcription sites (TSs) (Femino et al., 1998; Zenklusen et al., 2008), was next employed (see Extended Experimental Procedures and Figures S3A, S3B, and S3E). Single TS was detected in the nuclei of these haploid cells, using either the double probes (Figure 3B) or three dimensional (3D) reconstructions of cells labeled with the ORF probes (Movie S1). Most WT and Δ*xrn1* cells (88%) contained a TS, whereas only 66% of the *xrn1*^{D208A} cells contained a TS ($p = 2.6 \times 10^{-8}$) (Figures 3C and S3F and Movie S2).

WT cells contained TSs with more than one transcript (equivalent to multiple elongating Pol II occupancy) (Figures 3C and S3)—indicative of frequent transcription initiation or reinitiation events (Zenklusen et al., 2008). In contrast, Δ*xrn1* and *xrn1*^{D208A} cells contained TSs with only one transcript (Figures 3C and S3F), suggesting that Xrn1p is required for either transcription initiation, elongation, or both. Reassuringly, despite the transcriptional defects, *TEF4* mRNA number per WT cell was comparable to that in the mutant cells, as determined by both FISH and northern analyses (Figures S3C and S3D, respectively). Note that nuclear export of the *TEF4* mRNA in both *xrn1* mutant strains was normal, as no nuclear accumulation could be observed by FISH analysis outside the TS context (Figure 3B, Movies S1 and S2 and data not shown).

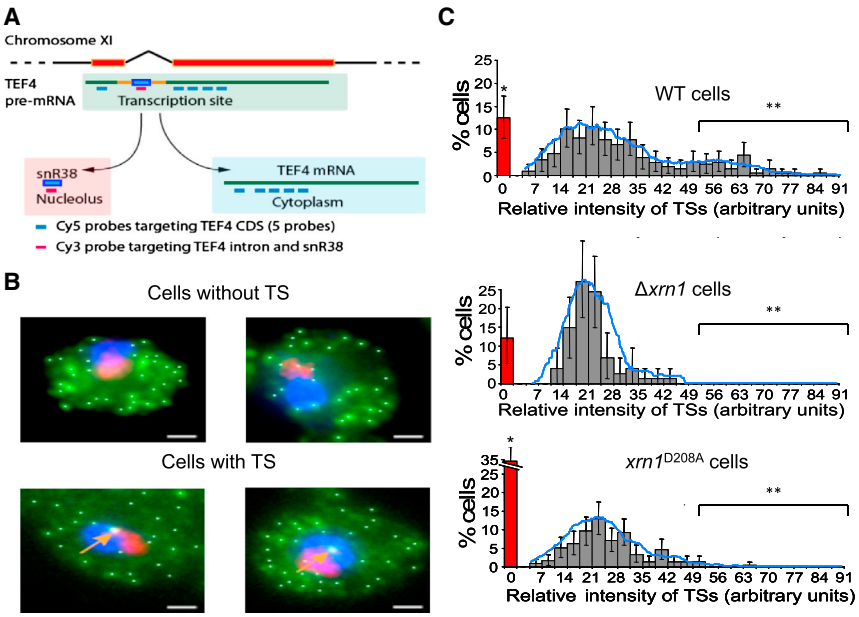

Figure 3. Xrn1p Affects Pol II Occupancy on *TEF4* Gene

(A) Schematic representation of the FISH approach and the position of the six probes.

(B) Merged FISH images of several representative cells with or without TSs. Images of *TEF4* Cy5 labeled probes, *snR38* Cy3 labeled probe, DAPI (pseudocolored green, red, and blue, respectively) and spot centroids (white dots; see Figure S4A) were merged into single images. Arrows indicate TSs. The large red area is the nucleolus.

(C) Frequency of cells (y axis) as a function of *TEF4* TSs intensities. Error bars represent 95% confidence intervals. See Figure S3E for interpretation. *p = 2.6 × 10^{-8} between WT and *xrn1*^{D208A}; **p < 10^{-4} between WT and both *xrn1* mutants.

See also Figure S3 and Movies S1 and S2.

Various mRNA Decay Factors Shuttle between the Cytoplasm and the Nucleus in a Manner Dependent on Proper mRNA Decay

The studied DFs are detected by and large in the cytoplasm (e.g., Teixeira and Parker, 2007). By inactivating export using a temperature-sensitive strain (Brune et al., 2005), we found that all tested DFs accumulated in the nucleus, like Pab1p that served as the positive control (Brune et al., 2005). Because nuclear accumulation was independent of de novo translation (Figures 4A and S4A), we conclude that the same protein molecules, which had been present in the cytoplasm prior the heat inactivation, entered the nucleus. Nuclear accumulation of Pat1p and Dhh1p was previously observed in a Δ*lsm1* strain (Teixeira and Parker, 2007), suggesting that these DFs are exported in complex with Lsm1p. Thus, all the examined DFs normally shuttle between the two compartments. We suspect that these DFs are usually visualized in the cytoplasm because their export rate exceeds their import rate. Interestingly, the equilibrium between export and import kinetics could be altered in response to environmental cues such as starvation (Figures S4B–S4E and S4G) or HS (Figure S4F). Furthermore, nuclear accumulation of some of the examined DFs could be detected in several WT strains under optimal conditions (Figures S4B and S4C).

In order to assess whether nuclear import of DFs is dependent on proper mRNA decay, the same shuttling assay was performed using various *XRN1* mutants. Import of Xrn1^{D208A}p-GFP was severely impaired (Figure 4B). Xrn1^{D208A}p binds decapped RNAs normally, without degrading them (Solinger et al., 1999). We hypothesized that the combination of these two features might block its import. To test this hypothesis, we introduced a second mutation in the pocket that binds the decapped RNA. Two such mutations were employed, R101G and H41D (Jinek et al., 2011; Page et al., 1998), which cause little effect on the proliferation rate (Figure S1E). Remarkably, introducing the R101G mutation into Xrn1^{D208A}p partially restored import capacity of this (still enzyme dead) protein, suggesting that the RNA needs to be positioned properly in the active site in order to repress import of Xrn1^{D208A}p. However, import of Xrn1^{D208A,R101G}p-GFP was not as efficient as import of the WT Xrn1p-GFP (see p values in Figure 4B), raising the possibility that proper RNA binding is important, by itself, for efficient import. To examine this possibility, we determined the import capacity of Xrn1^{R101G}p-GFP and Xrn1^{H41D}p-GFP. Indeed, import of these proteins was similarly compromised relative to that of Xrn1p-GFP (Figure 4B, p = 0.01 and p = 0.02, respectively). Pab1p-GFP was efficiently and equally imported in all the strains, demonstrating that the import defects of the various *xrn1* mutant cells is not general. In summary, efficient import of Xrn1p requires both proper RNA binding in the active site and its subsequent degradation. Only WT Xrn1p is therefore imported efficiently.

Interestingly, Dcp2p-RFP import was severely impaired in *xrn1*^{D208A} cells (p = 0.01) but was relatively efficient in *xrn1*^{D208A,R101G}, *xrn1*^{R101G}, *xrn1*^{H41D}, or Δ*xrn1* cells (Figure 4C). Furthermore, during starvation, *xrn1*^{D208A} cells poorly imported various other DFs (Figure S4G). Collectively, these results suggest that import of DFs does not occur as a default. It seems to require normal Xrn1p that is capable of binding decapped RNA and executing 5′ to 3′ mRNA decay. As shown below, the import features of Xrn1p are correlated with its capacity to stimulate transcription.

Decay Factors Associate with Chromatin and Stimulate Transcription Initiation

Next, we examined whether DFs are capable of binding chromatin, using chromatin immunoprecipitation-exo (ChIP-exo) analysis (Rhee and Pugh, 2012). Due to the exonuclease activity that degrades most of the DNA molecules that were not covalently bound by the immunoprecipitated (IP-ed) proteins, binding peaks are more dispersed than standard ChIP-sequencing, yet with better resolution and better signal-to-noise ratio (Figures 5A and 5D). All the examined DFs (Xrn1p-TAP, Dcp2p-TAP, and Lsm1p-TAP) were detected along the chromatin at levels significantly higher than the control (Figures 5A and 5D).

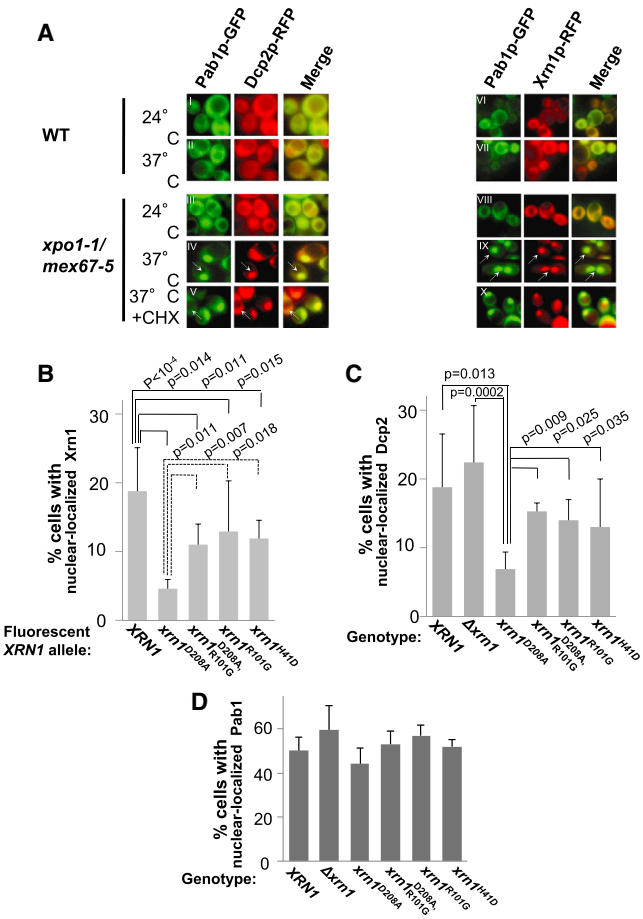

Figure 4. Factors of the major mRNA Decay Pathway Are Nucleocytoplasmic Shuttling Proteins, Whose Import Is Compromised by Mutating the Xrn1p Active Site

(A) WT cells or *xpo1-1, mex67-5* mutant cells coexpressing Pab1p-GFP and the indicated RFP fusion proteins were proliferated at 24°C and then shifted to 37°C for 1 hr (II, IV-V) or 2 hr (VII, IX-X). CHX, cycloheximide. For more details see Figure S4. Arrows indicate nuclear colocalization of Pab1p-GFP and RFP fusion proteins. The images in (IX) are a composition of two different fields.

(B–D) Import of Xrn1p and Dcp2p is dependent on Xrn1p exonuclease activity and on its 5′-phosphate binding. Δ*xrn1, xpo1-1, mex67-5* cells coexpressing *XRN1*-GFP or the indicated mutant derivative thereof and *PAB1*-RFP (B), or *DCP2*-RFP and *PAB1*-GFP (C), were subjected to the same assay as in (A), IX (for B) or IV (for C and D). Results of Pab1p-RFP, which was coexpressed with Xrn1p-GFP, and Pab1p-GFP that was coexpressed with Dcp2p-RFP, are shown in (D). Percentage of cells with nuclear localization was determined. Mean values ± SD are shown (n > 100). p values of any pairwise difference that was <0.05 is indicated. All other differences were statistically insignificant. See also Figure S4.

Remarkably, all three DFs, unlike the control, preferentially bind ~30 nucleotides upstream to transcription start sites (TSs) (Figure 5B), the site where the transcription preinitiation complex (PIC) is assembled (Kornberg, 2007). Moreover, efficiency of their binding to promoters is correlated with transcription rate, determined by GRO (Figure 5C). These two results suggest that chromatin binding is transcriptionally functional.

Xrn1p-TAP and Lsm1p-TAP produced almost overlapping ChIP peaks along *PMA1* gene locus (Figure 5D) and in other loci (Figure 5A and data not shown). Dcp2-TAP profile was similar to that of the other two DFs but not identical. These data suggest that DFs do not bind chromatin as independent factors. Rather, at least Xrn1 and Lsm1 seem to bind as a complex.

To corroborate DF binding to chromatin, we also performed a ChIP assay followed by qPCR analysis (Figure 5E). Binding of Xrn1-TAP along *PMA1* was similar to the binding profile obtained by the ChIP-exo technique (compare Figure 5D with 5E). Xrn1p-TAP was also found to be associated with the *TEF4* promoter as well as with other promoters (data not shown), but not with rDNA (Figure S5A). Moreover, the ChIP-qPCR indicates that not only Xrn1p, Lsm1p, and Dcp2p bind promoters, but also Pat1p-TAP, and Dhh1p-TAP are capable of binding promoters (Figures S5B and S5C). Consistent with a direct binding to the chromatin, ChIP-qPCR signals of Xrn1p-TAP and Dcp2p-TAP did not decrease due to RNase digestion prior to IP (data not shown). We found that import of Dcp2p is defective in *xrn1*^{D208A} cells (Figure 4C). Consistently, less Dcp2p-TAP was found associated with *PMA1* promoter in *xrn1*^{D208A} cells compared to WT cells (44% ± 3% in the mutant compared to the WT) (data not shown).

Our results so far suggest that DFs interact with PIC and are involved in transcription initiation. To further corroborate this role, we examined whether they are capable of stimulating transcription when artificially recruited to reporter promoters (Titz et al., 2006). We fused the DFs to the Gal4p DNA-binding domain (Gal4p-BD), which also possesses a strong nuclear localization signal (NLS), and analyzed transcriptional activation of the reporter genes, P_{GAL1}-*HIS3* and P_{GAL7}-*lacZ* as well as the natural *GAL10* gene.

Transcription of these genes was stimulated by recruitment of some of the DFs to their promoters, using the Gal4p NLS and DNA-binding capacity (Figures S5D–S5G and Table S5). Interestingly, Gal4p-BD-Dcp2-4p, a mutant lacking decapping activity, activated transcription similarly to Gal4p-BD-Dcp2p (Figures S5D, S5E, and S5G and Table S5). This suggests that the decapping activity of Dcp2p per se is not necessary for its capacity to stimulate transcription.

Although we showed that many DFs shuttle between the cytoplasm and nucleus as well as associate with chromatin, not all were able to activate transcription. This may either reflect a true biological feature (i.e., they do not contain an "activating domain") or may be due to differences in expression levels of the fusion genes (Figures S5H and S5I; see legend for discussion) or the effect of the Gal4p-BD moiety.

In a strain harboring the *xrn1*^{D208A} mutation (Figure S5F) or Δxrn1 (data not shown), Gal4p-BD-Dcp2p was unable to induce transcription. However, Gal4p-BD fusion of Ccr4p, Pat1, and Rpb3p activated transcription in this mutant, suggesting that Xrn1p is specifically required for transcriptional activation by Gal4p-BD-Dcp2p. Taken together, these results, combined with the role assigned to these factors in transcription and their chromatin-binding features, argue against a trivial effect of DFs in this tethering assay.

Decay Factors Affect Transcription Elongation

Unexpectedly, our GRO analysis revealed a direct correlation between the negative impact of Xrn1p disruption on transcription

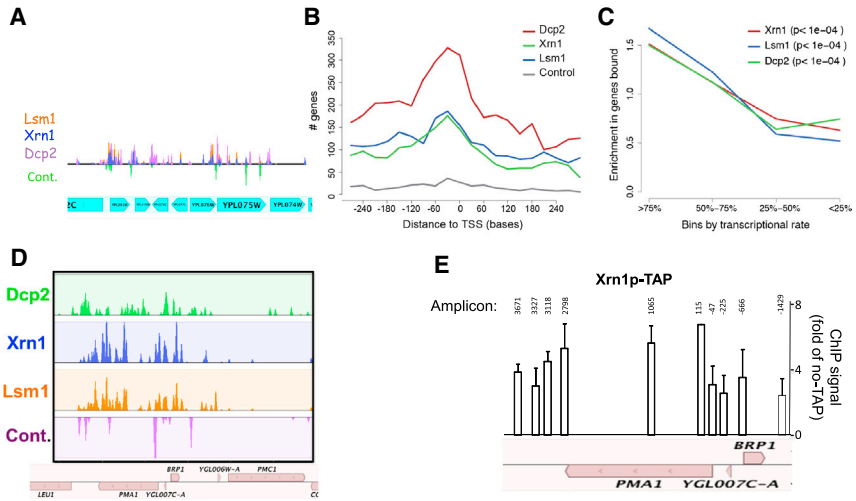

Figure 5. Factors of the Major mRNA Decay Pathway Associate with Chromatin of Transcriptionally Active Genes

(A) Association of Xrn1p, Dcp2p and Lsm1p across the chromatin. A MochiView representation of normalized ChIP-exo data of the indicated DFs. A snapshot view of a small genomic region, as indicated below, is shown.

(B) The ±300 bp region around the promoter was divided into 11 windows (x axis). For each of the indicated libraries, we computed the number of genes that had ten or more counts in each of the windows (y axis).

(C) Binding of DFs to promoters is correlated with TR. Genes were divided into four groups based on their TR (the most highly transcribed group is defined as ">75%"). The ratio of the observed versus expected number of genes bound in promoter regions, defined as ±300 bp of TSs by the indicated DF is shown (x axis). p values were computed empirically doing 10,000 permutations were we randomly shuffled binding data.

(D) Association of TAP-tagged DFs with chromatin at *PMA1* locus and vicinity. MochiView representation, as in Figure 5A. ORFs are depicted at the bottom. Control samples in (A)–(D) represent cells that carry no tagged gene.

(E) ChIP-qPCR analysis of WT cells expressing Xrn1p-TAP or control cells without TAP (No-TAP) was performed and analyzed by qPCR with the indicated amplicons. Mean values of four biological repeats normalized to the input signal, No-TAP signal and an internal *lacZ* spike ± SD are shown.

See also Figure S5.

and the open reading frame (ORF) length (Figure 6A), raising a possible role in transcription elongation (Morillo-Huesca et al., 2006; Rodríguez-Gil et al., 2010). To examine this possibility further, we first used our previously developed assay to examine the distribution of either Pol II molecules by means of RNA polymerase ChIP-on-chip (RPCC), or the distribution of transcriptionally active Pol II by means of GRO (Rodríguez-Gil et al., 2010). We used a membrane containing 5′ and 3′ probes that enabled us to determine how Pol II molecules or Pol II activity are distributed in the 3′ portions relative to the 5′ portions of these ORFs. RPCC data revealed abnormal Pol II accumulation in the 3′ portion of the mutant genes. In contrast, we observed no such bias in the GRO signal (Figure 6B, red columns), indicating that these surplus Pol II molecules were unable to elongate transcription in vitro.

We next similarly examined Pol II occupancy and its activity along the *GAL1* gene after induction by galactose. Consistent with the genomic data shown in Figure 6B, Pol II occupancy increased by disruption of Xrn1p (Figure 6C), whereas its elongation activity, as determined by run-on, did not (Figure S6A). Specifically, the ratio between run-on signals in the mutant versus WT was maintained in the 5′ (arbitrarily defined as 1), middle, and 3′ portion of the gene (Figure S6A). Phosphorylation of Pol II CTD heptad repeat at Ser-2 position is one hallmark of elongating Pol II (Bataille et al., 2012; Meinhart et al., 2005). Consistent with a role for Xrn1p in elongation, Ser-2 was hypophosphorylated in *xrn1* mutants compared to WT cells (Figure 6C).

The drug 6-azauracil (6-AU) depletes NTPs thereby reducing both the elongation rate and Pol II processivity, which is aggravated by mutations in elongation factors (Mason and Struhl, 2005). Therefore, 6-AU sensitivity is often indicative of a defect in transcription elongation (e.g., Fish and Kane, 2002; Hartzog et al., 1998; Malagon et al., 2006; Mason and Struhl, 2005). Indeed, some decay mutants were hypersensitive to 6-AU (Figure S6B), reinforcing our conclusion that they are involved in transcription elongation.

Transcription Is Linked to mRNA Decay

Our finding that transcription is severely compromised upon disruption of Xrn1p enzymatic activity suggests that the role of Xrn1p in transcription is mechanistically linked to its role as RNA exonuclease. To examine this possibility, we first analyzed whether the binding capacity of Xrn1-TAP, Lsm1-TAP, and Dcp2-TAP to promoters, determined by ChIP-exo, is correlated with the effect that Xrn1p disruption has on transcription, determined by GRO. We arbitrarily divided the genes into four equal groups based on the effect that Xrn1p disruption had on their transcription and found a direct correlation with promoter binding (Figure 7A). This correlation reinforces our premise that binding of Xrn1p (and possibly also Dcp2p and Lsm1p) to chromatin is related to its effect on transcription. Moreover, we found that promoter binding is also correlated with HL (Figure 7B). Interestingly, the studied DFs tend to bind promoters of genes that encode unstable mRNAs ($p < 0.005$) establishing a linkage between promoter binding and mRNA decay. If the two functions are indeed linked, one expects that a defect in one function would affect the other. To test this possibility, we arbitrarily classified the mRNAs according to the effect of Xrn1p disruption on their decay rate (DR), and examined the transcriptional effect that Xrn1 disruption has on these groups. Remarkably, we found a direct correlation between the capacity of the cells to degrade mRNAs and to synthesize them (Figure 7C). This conclusion is also implied by the data in Figure 1C. Note that *xrn1*^{D208A} cells are more defective in transcription than Δ*xrn1* cells (Figure 2A, S2A and S2E). As shown in Figure 7C, for any given strain and among the strains, the more mRNA decay is dependent on

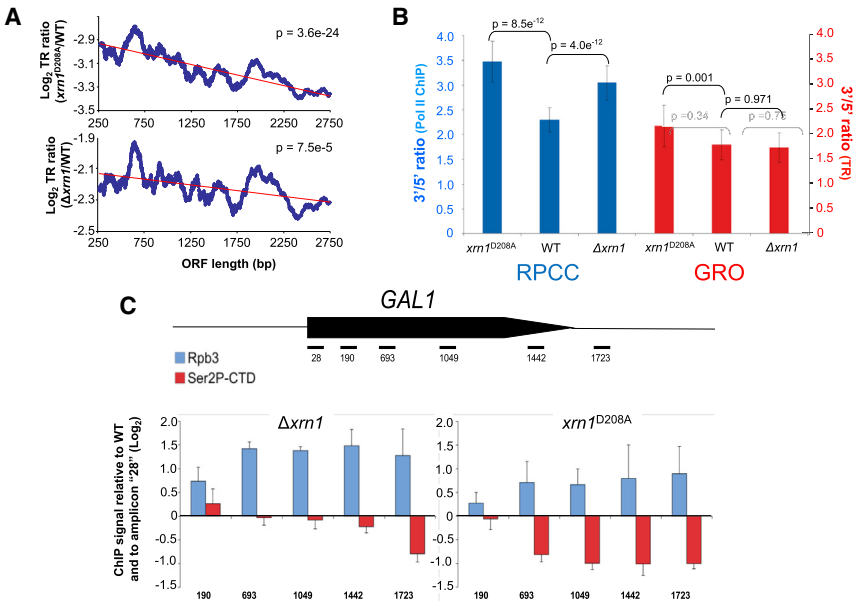

Figure 6. Factors of the Major mRNA Decay Pathway Affect Transcription Elongation

(A) The impact of *XRN1* disruption on transcription is proportional to the ORF length. Sliding window analysis of the dependence of the change in TR ratio (mutant/WT) on ORF length. TR ratios in $\log_2$ scale (Table S4) were averaged using a 200 gene sliding window. The red line shows the fitted linear negative tendency. The p values shown at the top were obtained by t test determining the differences in average TR ratio between the genes of <1,000 bp and those >1,750 bp.

(B) 3′/5′ RPCC (blue columns) and GRO (red columns) analyses were performed as described in Experimental Procedures. The histograms depict the average ratio of 3′/5′ signals obtained for any of the indicated strains ± SD of three independent experiments. A Wilcoxon test shows that the medians of the distributions are different for total Pol II molecules but not for elongating ones.

(C) $\log_2$ representation of Pol II (pulled down by anti-Rpb3p antibodies) and Ser-2-phosphorylated CTD (Ser2P-CTD) ChIP signals at the indicated positions along *GAL1* in cells grown in galactose medium. Data are expressed relative to amplicon "28," followed by normalization of each value to the corresponding position in the WT strain, which was defined as "1." Mean values and SD of three independent experiments are shown. See also Figure S6.

Xrn1p, the more its synthesis is affected by disrupting its activity. Collectively, the capacity of Xrn1p to degrade mRNAs is related to its capacity to stimulate their synthesis.

Last, if the function of Xrn1p in transcription is linked to its function in mRNA decay, it might be possible to uncouple these two roles. We examined whether mutating either (1) the enzymatic activity (D208A) or (2) the pocket in the active site that binds the decapped 5′P-RNA (R101G) can uncouple the two functions. Unlike R101G, the D208A does not interfere with the normal RNA binding (Jinek et al., 2011; Page et al., 1998; Solinger et al., 1999). As expected (see Figure 2A), *xrn1*^{D208A} cells displayed defective transcriptional induction of *GAL* genes in response to galactose. Accumulation of mRNA upon similar stimulation of Δ*xrn1* and *xrn1*^{R101G} strains with galactose was comparable to that in the WT cells (Figure 7D). Because *xrn1*^{R101G} and Δ*xrn1* strains exhibit identical mRNA decay rates (Figure S7A) and accumulation of *GAL* mRNAs (Figure 7D), and because Δ*xrn1* cells are defective in transcription of most genes (Figure 1D), we can conclude that transcription in *xrn1*^{R101G} strain is as defective as it is in Δ*xrn1* strain. These results suggest that proper recruitment of decapped RNA to Xrn1p active site is important for the capacity of Xrn1p to regulate transcription because it is important for its import (Figures 4B and 4C). Remarkably, introducing the R101G mutation into *xrn1*^{D208A} partially recovered the severe transcription defect exhibited by the *xrn1*^{D208A} strain. Consequently, the transcription capacity of the *xrn1*^{D208A,R101G} strain was similar to that of the Δ*xrn1* and *xrn1*^{R101G} strains (Figure 7D), given that mRNA decay in these three strains was identical (Figure S7A) (see Discussion).

Collectively, the four independent results, presented in Figure 7, suggest that the capacity of Xrn1p to bind and degrade mRNAs is related to its capacity to stimulate their synthesis. The hitherto first and the last stages of the mRNA life are therefore interconnected (Figure 7E).

Discussion

Our work and those of others demonstrate that the steady-state mRNA levels cannot serve as a reliable assay to examine transcription or decay rates. These levels are robust to perturbations in either transcription (Esberg et al., 2011; Goler-Baron et al., 2008; Harel-Sharvit et al., 2010; Schwabish and Struhl, 2007) or mRNA decay (this work). Here we show that most mRNAs in optimally proliferating yeast cells are degraded by the 5′ to 3′ exonuclease Xrn1p, as proposed previously (Anderson and Parker, 1998; Coller and Parker, 2004). Nevertheless, disruption of the major decay pathway does not result in elevated steady-state levels; in most cases these levels were even decreased. Consistently, disruption of this pathway has a minor effect on the proliferation rate of optimally proliferating cells (Figure S1E). We propose that this robustness is maintained by the dual role of the "decaysome" in mRNA synthesis and decay.

Decay Factors Play a Direct Role in Transcription

The cross talk between mRNA synthesis and decay involves a role of DFs in transcription. The following observations are consistent with a direct role in transcription. (1) Binding of Pat1p-TAP, Dhh1p-TAP, Xrn1p-TAP, Dcp2p-TAP, and Lsm1p-TAP to promoters, and to a lesser extent also to other regions of transcription units (Figure 5). Their binding to promoters seems to be transcriptionally relevant (see below). Chromatin binding is consistent with the shuttling of these factors back and forth between the nucleus and the cytoplasm. (2) The GRO data clearly demonstrate that densities of active Pol II are adversely affected by deleting Xrn1p or by mutating its active

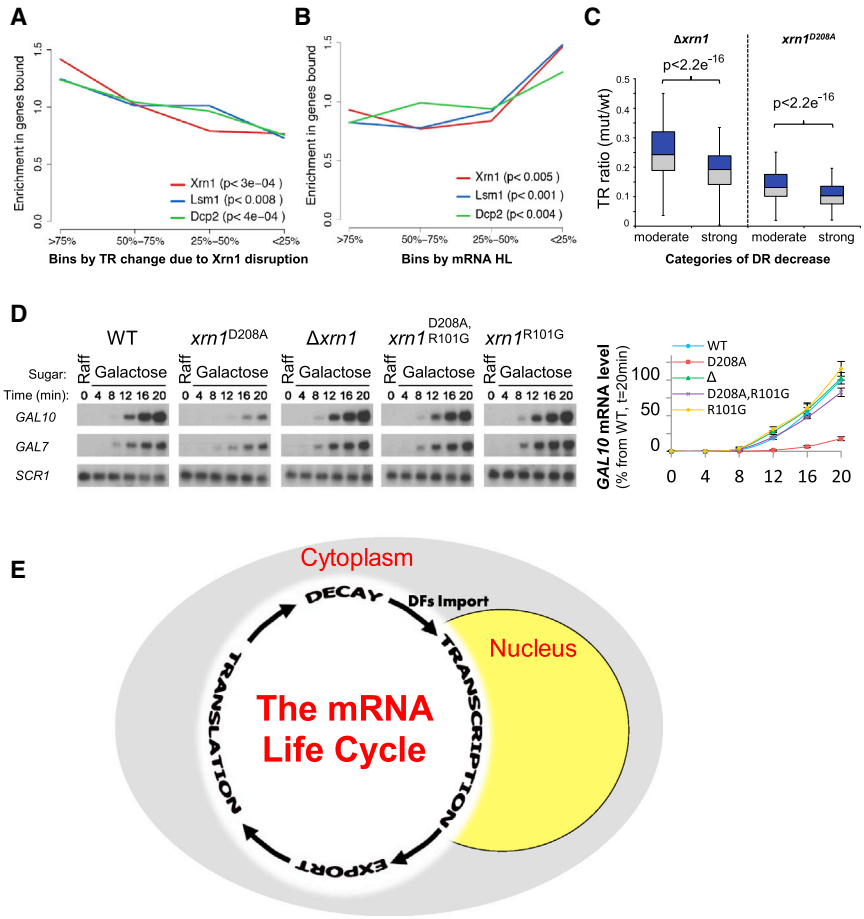

Figure 7. Coordination between Transcription and Decay

(A) Binding of DFs to promoters is correlated with the effect of xrn1 disruption on transcription.

(B) Binding of DFs to promoters is correlated with HL (for list of HLs see Table S4). For (A) and (B), see analysis of ChIP-Exo data in Extended Experimental Procedures.

(C) A correlation between mRNA stability and synthesis is observed by disrupting *XRN1*. Box plot representation of the median and 2nd and 3rd quartiles of the changes in transcription rate (TR) of two gene categories: moderate decrease in degradation rate (DR) and strong decrease in DR (see Table S4). DR was calculated as described in Extended Experimental Procedures. The whiskers show the maximum and minimum of the data set, excluding the outliers, which lie beyond the 1.5 times the interquartile range. Distributions were found to be different using Wilcoxon statistical test as shown in the upper part at the indicated p value.

(D) Transcriptional induction of *GAL* genes was performed on the indicated strains as described in Figure 2A. Error bars represent SD of three assays. The Xrn1p proteins in the different strains were expressed from the centromeric plasmids pMC491, pMC492, pMC579 and pMC582, in Δ*xrn1* strain (yMC511).

(E) A conceptual model: gene expression is a circular process (see Discussion).

See also Figure S7.

site (e.g., Figure 1D). (3) Single-cell imaging technique demonstrates that mRNA synthesis is dependent on Xrn1p (Figures 3 and S3). The results of this approach are consistent with a role for Xrn1p in transcription initiation and elongation. (4) The effect of disrupting the enzymatic activity of Xrn1p or Dcp2p on the transcriptional induction of genes from several families. Although there is little difference between the effect of disrupting Xrn1p enzymatic activity and its complete deletion on mRNA HL (Figure S1C), the two mutations have different effects on transcription (e.g., Figure 2A). This indicates that the presence or absence of Xrn1p or Dcp2p, regardless of their enzymatic activities or their effect on mRNA decay, affects Pol II transcription. (5) The tethering assay that shows that some DFs may have an "activating domain" (Figures S5D–S5G). (6) The numerous genetic and physical interactions of DF genes or proteins with many components of the transcription apparatus (Figure S1B and Table S3). (7) The paradoxical effect that deletion of DF genes has on mRNA levels. Importantly, this paradoxical effect results from deleting any of the many DFs we tested (Figures 1A and S1A). This observation suggests that the crosstalk between mRNA synthesis and decay is not specific to some factors. Rather, it is a feature of the decaysome complex.

Whole-genome-binding features of Xrn1p-TAP, Dcp2p-TAP and Lsm1p-TAP helped us reveal additional linkages between the two roles of the decaysome. The three studied DFs prefer to bind ~30 bp upstream of TSs (Figure 5B). Because the PIC also binds ~30 bp upstream of TSS (Kornberg, 2007), it is possible that the three studied factors assemble together with the PIC. This possibility is in accord with the numerous physical and genetic interactions between DFs and transcription factor IID (TFIID), and Spt-Ada-Gcn5-Acetyl transferase (SAGA) and the mediator complexes (Figure S1B and Table S3). Xrn1p-TAP, Dcp2p-TAP, and Lsm1p-TAP prefer to bind promoters of genes whose transcription is highly affected by Xrn1p disruption (Figure 7A), again suggesting that promoter binding is transcriptionally functional. Moreover, these DFs prefer to bind promoters that govern transcription of unstable mRNAs (Figure 7B), suggesting a linkage between their roles in mRNA decay and transcription (we therefore do not expect binding of DFs to all PICs or all transcription units). These preferences highlight the linkage between DFs roles in the two mechanisms. Detailed mechanistic understanding of these preferences remains to be determined.

Xrn1p Functions Also in Transcription Elongation

Deletion of *XRN1* or disruption of its exonuclease activity leads to accumulation of transcriptionally incompetent Pol II at the 3′ portions of ORFs (based on the apparent discrepancy between RPCC and GRO data in Figure 6), which is also hypophosphorylated. When Pol II encounters nucleosome or other obstacles, it

reverses its direction and backtracks, leaving the transcript 3′-end misaligned with the active site and therefore cannot polymerase any further (Cheung and Cramer, 2011). Accumulation of inactive Pol II molecules is a hallmark of backtracking Pol II (Gómez-Herreros et al., 2012; Pelechano et al., 2009; Pérez-Ortín et al., 2012; Rodríguez-Gil et al., 2010). A main function of transcription factor IIS (TFIIS) is to release backtracked Pol II, thus helping it to traverse through nucleosomes, and its deletion leads to accumulation of Pol II within the first four nucleosomes (Churchman and Weissman, 2011). Notably, deleting TFIIS or some other elongation factors results in accumulation of Pol II in 5′ portions of ORFs, whereas deleting others—in 3′ portions (Churchman and Weissman, 2011; Kruk et al., 2011; Mason and Struhl, 2005; Rodríguez-Gil et al., 2010). Indeed, deleting *DST1* encoding TFIIS leads to defective transcription driven by Gal4p-BD-Rpb3p and Gal4-BD-Dcp2p in the tethering assay (data not shown). The mechanism underlying the second group of elongation factors, among them are Ssd1p and Bur2p (Rodríguez-Gil et al., 2010), is relatively little understood. As shown in Figure 6, Xrn1p belongs to the second, less studied, group. Interestingly, we and other investigators have found that Ccr4p-Not complex also belongs to the second group (Kruk et al., 2011; Rodríguez-Gil et al., 2010), raising the possibility that Xrn1p and Ccr4p-Not play a role in a common proteinacious context. In agreement with this line of thought, deleting *DST1* did not compromise transcription driven by Gal4p-BD-Ccr4p, Gal4p-BD-Pat1p, and Gal4p-BD-Dhh1p in the tethering assay (data not shown). Our data are consistent with a model whereby some DFs prevent Pol II from backtracking, thereby stimulating elongation in a manner independent of TFIIS (see also Kruk et al., 2011). Consistently, *PAT1*, *LSM1*, and *CCR4* are synthetically lethal with *DST1* (Table S3), suggesting that transcription elongation requires at least one of the pathways, either the TFIIS-dependent or the alternative pathway—mediated by some DFs. In recent years, it has become clear that recruiting Pol II to transcription start sites is insufficient to promote transcription and that postinitiation stages play key roles. The roles of DFs in elongation add an additional level of complexity to the regulations that occur after transcription begins.

Decay Factors Might Function in Transcription as a Complex or Subcomplexes

A number of observations led us to conclude that the novel transcriptional role is not restricted to a limited number of DFs. (1) Disruption of any DF that we examined has downregulated transcription. (2) All the examined DFs are shuttling proteins. Shuttling of some DFs is affected by disruption of Xrn1p enzymatic activity, suggesting that some of them shuttle as a complex. (3) Tethering a number of DFs to promoters stimulates transcription, which in some cases is dependent on Xrn1p or other DFs (Figure S5F and data not shown), suggesting cooperation between more than one DF. (4) All five DFs that we tested bind promoters. A whole-genome ChIP association of three of them showed a preference to coassociate ~30 bp upstream of TSS. (5) Very similar ChIP profiles along genes also suggest that the DFs do not bind chromatin as independent factors.

The Linkage between mRNA Decay, Import of Decay Factors and Transcription

DFs play two opposing roles in determining mRNA levels. Significantly, these two activities seem to be mechanistically linked (Figures 7B and 7C). Our data raise the possibility that DF import plays a key role in this linkage. A positive correlation is found between transcriptional efficiency and the capacity of Xrn1p and other DFs to shuttle as well as to degrade mRNAs. First, proper binding of Xrn1p to the decapped RNA is required for its efficient import (Figure 4B) and for efficient transcription (Figure 7D). Second, cells harboring $xrn1^{R101G}$, $xrn1^{H41D}$, $xrn1^{D208A,R101G}$, or a deletion of *XRN1*, which can import DFs (other than Xrn1p) efficiently, transcribe better than those harboring $xrn1^{D208A}$ (e.g., Figure 7D), which are defective in importing $Xrn1^{D208A}$p as well as other DFs (Figures 4B, 4C and S4G). Because $xrn1^{D208A,R101G}$ cells transcribe better than $xrn1^{D208A}$ cells, it is clear that D208A mutation per se does not disrupt the ability of Xrn1p to function in transcription. Rather, D208A affects the interplay between the two opposing roles of Xrn1p in mRNA decay and transcription, most probably due to its severe effect on import. D208A, which disrupts the exonucleolytic activity, exerts its adverse effect only if the Xrn1p active site binds the RNA at the 5′ end properly. If it does not bind properly, e.g., in the case of R101G, the enzymatic activity is neutral (Figures 4B, 4C, and 7D). Thus, only the combination of properly binding the decapped RNA in the Xrn1p active site and the inability to degrade it blocks import of key DFs (including the Xrn1p mutant form itself) (see a model in Figure S7B). It is possible that the combination of D208A and R101G mutations displaces Xrn1p from its natural context, creating a situation comparable to complete absence of Xrn1p (Figures 4B, 4C, and 7D).

We propose a model (Figure S7B) whereby Xrn1p represses premature import of DFs, thus linking between mRNA decay and import. Efficient repression is dependent on proper binding of the decapped RNA in the 5′-phosphate-binding pocket of Xrn1p's active site. Only once the RNA has been successfully degraded does Xrn1p stimulate DF import, which is followed by transcriptional stimulation. According to this model, $Xrn1^{D208A}$p represses import constitutively, because the RNA in its active site is not degraded. Indeed, the RNA can be degraded by the exosome. However, a few bases may remain bound in Xrn1p-binding pocket, inaccessible to the exosome, maintaining Xrn1p in a conformation that represses import. The enzyme-dead Dcp2-4p, which severely compromises transcription (Figure 2C), might similarly block import as long as it is bound to the 5′-cap structure, an issue that remains to be examined.

Other Possible Mechanisms

The decaysome may affect transcription by degrading regulatory RNAs (e.g., ncRNAs) (Geisler et al., 2012; van Dijk et al., 2011). However, our current data are more consistent with a degradation-independent mechanism. (1) All DFs examined are shuttling proteins and bind chromatin. This binding is direct, and not mediated by RNA (data not shown), and is affected by disrupting the exonucleolytic activity of Xrn1p (see earlier). (2) Some DFs prefer to bind directly at the PIC assembly site (Figure 5B) and can activate transcription when artificially tethered to promoters

(Figures S5D–S5G and Table S5). (3) DFs are required for transcriptional activation (as well as for the decay) of ncRNAs in a manner similar to that of mRNAs (Figures S2G–S2I). (4) Transcription and/or decay of ncRNAs seems to relate mostly to environmentally induced genes and involves only Xrn1p or Dcp2p (Geisler et al., 2012; van Dijk et al., 2011), whereas we show that transcription of most genes, including housekeeping ones, is affected by DFs (Figures 1 and S1). (5) Most genes that undergo changes in intragenic Pol II distribution in response to Xrn1 disruption lack Xrn1-dependent noncoding RNAs (XUTs) (data not shown). (6) The transcriptional capacity of cells expressing the enzyme-dead Dcp2-4p or Xrn1^{D208A}p is different than those carrying a deletion of *DCP2* or *XRN1* (Figures 2, S2, 3, and 7). This difference is inconsistent with a simple decapping and degradation of ncRNA as the main underlying mechanism. Indeed, the transcriptional capacity of *xrn1*^{D208A} cells can be partially rescued by introducing another mutation (R101G), indicating that the active site per se is not critical for transcription (Figure 7D). Moreover, inactivating the enzymatic activity of Dcp2p, using Dcp2-4p mutant form, does not affect the protein capacity to activate transcription in the tethering assay (Figures S5D, S5E and S5G and Table S5), suggesting that the decapping activity of Dcp2p is not necessary for its capacity to stimulate transcription in this assay.

Nevertheless, it is quite possible that the effect of the decaysome on mRNA synthesis involves more than one mechanism, a general and direct one described here, and one that acts indirectly through degradation of ncRNA, which may be restricted to subclasses of genes. Some of our unpublished observations suggest that the relative impact of the two mechanisms is strain dependent (G.H. and M.C., unpublished data).

Gene Expression Is Circular

The capacity of the decaysome to stimulate both mRNA synthesis and decay probably helps coordinating the two activities that determine mRNA levels. A whole-genome analysis demonstrated that families of yeast genes, whose transcription is coregulated in response to environmental cues, are also degraded in a coordinated fashion, maybe by a common mechanism (Shalem et al., 2008). The dual role of the decaysome may underlie this coordination. An interesting issue for future studies is how the balance between the synthetic and decay functions of the decaysome is regulated. This kind of regulation can affect the fine-tuning of the desired steady-state levels, as well as the kinetics with which they are achieved in response to environmental changes.

Coupling of two processes, as we view it, requires that the activity of certain factor(s) in the first process is a prerequisite for its function in the subsequent step. Following this criterion, it was previously found that mRNA decay is coupled to translation, which, in turn, is coupled to mRNA export, maturation, and transcription (reviewed in Komili and Silver, 2008). Gene expression was therefore considered a linear pathway. Remarkably, Pol II, promoters and other transcription components can control cytoplasmic mRNA decay (Bregman et al., 2011; Dahan and Choder, 2013; Goler-Baron et al., 2008; Haimovich et al., 2013; Pérez-Ortín et al., 2013; Shalem et al., 2011; Trcek et al., 2011). The synthetic and decay processes can therefore be viewed as two arms of a larger machinery, the "synthegradosome." The coupling between the two arms of the synthegradosome converts gene expression into a circular system (Figure 7E). Circular processes are inherently robust, because defects in one stage affect the overall pace of the entire process, thereby maintaining the essential balance between the stages. The maintenance of mRNA levels is one manifestation of this principle.

EXPERIMENTAL PROCEDURES

Yeast Strains and Plasmids

Lists of yeast strains, plasmids, and construction details can be found in Tables S6 and S7 and Extended Experimental Procedures.

Yeast Cultures

Yeast cells were proliferated in synthetic complete medium (SC) at 30°C unless otherwise indicated. For starvation experiments, cells were incubated in media lacking carbon source and amino acids. For nucleocytoplasmic shuttling assay, cells were grown at 24°C and subsequently incubated at 37°C for 1–2 hr as indicated. For proliferation assay on 6-AU plates, 6-AU (100 μg/ml) was added to SC-Ura plates. Cells were serially diluted 1:5, spotted on the plates and incubated for 2 days at 28°C prior to photography. For proliferation of 3-AT plates, cells were streaked on SC-Trp-His plates containing different 3-AT concentrations (between 0 to 200 mM). Growth was assessed after 4 days. For more details see Extended Experimental Procedures.

Analysis of Steady State mRNA Level, mRNA Half-Life, and Transcription Induction/Repression

To determine RA and HL, cells were grown in synthetic complete (SC) medium at 30°C to 1 × 10^{7}cells/ml. To determine HL of specific mRNAs (Figure 1B), 1, 10-phenanthroline (100 μg/ml) (Merck) was used to block transcription.

For transcriptional induction and repression, using galactose and glucose respectively, cells were grown in SC-Raf (2% raffinose as carbon source) for at least seven generations until 5 × 10^6 cells/ml were present. Cell aliquot was taken for time point "0," followed by addition of 2% galactose. Cell aliquots were taken, as indicated. At 75 min, the remaining culture was washed twice with water at room temperature and then resuspended in preheated (30°C) SC containing 4% glucose. For the heat shock experiments, cells were shifted rapidly from 30°C to 42°C then incubated at 42°C for 30 min. Cultures were then rapidly cooled in ice water back to 30°C. For all experiments, samples in each condition were collected at the indicated time points. RNA extraction and northern blot analysis were performed as previously described (Lotan et al., 2005).

Fluorescence Microscopy

Fluorescence microscopy was performed as previously described (Lotan et al., 2005).

Fluorescent In Situ Hybridization

FISH probes were designed as described previously (Levsky et al., 2002). FISH was performed essentially as described (Zenklusen et al., 2008). Images were analyzed by a 2D Gaussian fit algorithm as previously described (Thompson et al., 2002; Zenklusen et al., 2008). A detailed protocol, including image acquisition, data analysis, 3D reconstructions, and statistical analysis can be found in Extended Experimental Procedures.

Genomic Run-On, 3′/5′ Ratio Analysis, Determining HLs and RNA pol II ChIP on Chip Experiments

Genomic run-on (GRO) analysis (three independent experiments) was performed as previously described (García-Martínez et al., 2004; Pelechano and Pérez-Ortin, 2010), with modifications (García-Martínez et al., 2011) using an updated version of the nylon microarrays (Alberola et al., 2004). 3′/5′ ratio analyses and RPCC were performed essentially as previously described (Pelechano et al., 2009; Rodríguez-Gil et al., 2010). Thiolutin

shutoff analysis was done as previously described (Pelechano and Pérez-Ortín, 2008). RPCC was done as described (Pelechano et al., 2009; Rodríguez-Gil et al., 2010). Run-on of *GAL1* was performed as described (Rodríguez-Gil et al., 2010). Detailed protocols can be found in Extended Experimental Procedures.

Chromatin Immunoprecipitation

Recruitment of TAP-tagged proteins to chromatin was assayed by ChIP analysis as previously described (Buck and Lieb, 2006) with some modifications: Crosslinking was performed at 0.75% formaldehyde; Spin-X centrifuge tube filters were used to prevent contamination from the IgG beads; elution buffer was spiked with an exogenous *lacZ* DNA fragment, which was later used to determine recovery during subsequent stages. The Absolute blue SYBR Green ROX mix (Thermo Scientific) was used for qPCR according to the manufacturer's instructions in a 10 μl reaction volume. qPCR was performed in Rotor-Gene 6000 (Corbett Life Science, Sydney, Australia). Detailed protocols can be found in Extended Experimental Procedures. ChIP-exo of TAP tagged proteins was performed by Peconic LLC (State College, PA). As a control, we used an isogenic strain that carries no tagged gene. Analysis of ChIP-Exo data and correlation to other genomic data sets are detailed in Extended Experimental Procedures.

Statistical Analysis

χ^2 test and standard t test were used for nuclear localization and β-gal assays, respectively, followed by p value calculations using GraphPad Software (http://www.graphpad.com/quickcalcs/pvalue1.cfm). Statistical analyses of GRO, FISH and ChIP data are detailed in the Extended Experimental Procedures.

Accessions Numbers

Gene Expression Omnibus (GEO) database references are GSE44312 for ChIP-exo data, GSE29519 for genomic macroarray data, and GSE43605 for 5'/3' portions of 384 genes macroarray data.

SUPPLEMENTAL INFORMATION

Supplemental Information includes Extended Experimental Procedures, seven figures, seven tables, and two movies and can be found with this article online at http://dx.doi.org/10.1016/j.cell.2013.05.012.

ACKNOWLEDGMENTS

We thank Roy Parker, Tatjana Trček-Pulisic, Daniel Larson, and Robert Singer for critically reading the manuscript. Roy Parker, Wolf Heyer, Karsten Weis, Tien-Hsien Chang, Arlen Johnson, Shay Ben-Aroya, and Daniel Kornitzer generously shared strains and plasmids. We thank Laboratorio de Chips de DNA (S.C.S.I.E., Universitat de València) for the GRO and the 3′/5′ macroarrays and Daniel Larson for sharing algorithms. This work was supported by Israel Science Foundation (1283/07), Ministry of Health, and Rappaport Foundation (to M.C.), ANR JC 0118-01 and la Ligue (to X.D.), the Spanish MCINN and European Union ERDF (BFU2010-21975-C03-01 and BFU2010-21975-C03-02) to J.E.P.-O. and S.C., respectively, and the Regional Valencian Government (GV PROMETEO/2011/088) (to J.E.P.-O.) and from Junta de Andalucía (JA grants P07-CVI02623 and P08-CVI-03508) to S.C., MICINN GV and JA grants involve EDRF resources from the EU. DARPA D12AP00004 and Center for Excellence in Genome Science from the NHGRI 1P50HG006193 to M.G. G.H. is currently a recipient of the Gruss-Lipper family postdoctoral fellowship. D.A.M. is a recipient of a Santiago Grisolía fellowship from GV. G.M.-Z. is a recipient of a FPU MICINN fellowship. G.H. and M.C. conceived the main hypothesis. G.H. constructed strains and plasmids and performed and analyzed the transcription, decay and tethering experiments, shuttling assays, proliferation assays, and PBs analysis. S.Z.C. and X.D. designed, performed and analyzed the FISH experiments. D.A.M. and J.E.P.-O. designed, performed, and analyzed the GRO, RPCC and thiolutin shut-off experiments. G.H. and O.B. designed, performed, and analyzed the ChIP-TAP. G.Z.M and S.C. contributed to design 5′/3′ GRO and RPCC experiments. G.Z.M. and S.C. designed, performed, and analyzed the Pol II and phospho-ser-2 ChIP of *GAL1* in glucose and galactose. M.G. and M.C. analyzed the ChIP-exo data. G.H. and M.C. wrote the manuscript. J.E.P.-O. and S.C. critically read and edited the manuscript. M.C. coordinated the project.

Received: June 9, 2011
Revised: January 3, 2013
Accepted: May 7, 2013
Published: May 23, 2013

REFERENCES

Alberola, T.M., García-Martínez, J., Antúnez, O., Viladevall, L., Barceló, A., Ariño, J., and Pérez-Ortín, J.E. (2004). A new set of DNA macrochips for the yeast Saccharomyces cerevisiae: features and uses. Int. Microbiol. *7*, 199–206.

Anderson, J.S., and Parker, R.P. (1998). The 3′ to 5′ degradation of yeast mRNAs is a general mechanism for mRNA turnover that requires the SKI2 DEVH box protein and 3′ to 5′ exonucleases of the exosome complex. EMBO J. *17*, 1497–1506.

Badis, G., Saveanu, C., Fromont-Racine, M., and Jacquier, A. (2004). Targeted mRNA degradation by deadenylation-independent decapping. Mol. Cell *15*, 5–15.

Bataille, A.R., Jeronimo, C., Jacques, P.E., Laramée, L., Fortin, M.E., Forest, A., Bergeron, M., Hanes, S.D., and Robert, F. (2012). A universal RNA polymerase II CTD cycle is orchestrated by complex interplays between kinase, phosphatase, and isomerase enzymes along genes. Mol. Cell *45*, 158–170.

Bregman, A., Avraham-Kelbert, M., Barkai, O., Duek, L., Guterman, A., and Choder, M. (2011). Promoter elements regulate cytoplasmic mRNA decay. Cell *147*, 1473–1483.

Brune, C., Munchel, S.E., Fischer, N., Podtelejnikov, A.V., and Weis, K. (2005). Yeast poly(A)-binding protein Pab1 shuttles between the nucleus and the cytoplasm and functions in mRNA export. RNA *11*, 517–531.

Buck, M.J., and Lieb, J.D. (2006). A chromatin-mediated mechanism for specification of conditional transcription factor targets. Nat. Genet. *38*, 1446–1451.

Cheung, A.C., and Cramer, P. (2011). Structural basis of RNA polymerase II backtracking, arrest and reactivation. Nature *471*, 249–253.

Churchman, L.S., and Weissman, J.S. (2011). Nascent transcript sequencing visualizes transcription at nucleotide resolution. Nature *469*, 368–373.

Coller, J., and Parker, R. (2004). Eukaryotic mRNA decapping. Annu. Rev. Biochem. *73*, 861–890.

Dahan, N., and Choder, M. (2013). The eukaryotic transcriptional machinery regulates mRNA translation and decay in the cytoplasm. Biochim. Biophys. Acta *1829*, 169–173.

Dunckley, T., and Parker, R. (1999). The DCP2 protein is required for mRNA decapping in Saccharomyces cerevisiae and contains a functional MutT motif. EMBO J. *18*, 5411–5422.

Esberg, A., Moqtaderi, Z., Fan, X., Lu, J., Struhl, K., and Byström, A. (2011). Iwr1 protein is important for preinitiation complex formation by all three nuclear RNA polymerases in Saccharomyces cerevisiae. PLoS ONE *6*, e20829.

Femino, A.M., Fay, F.S., Fogarty, K., and Singer, R.H. (1998). Visualization of single RNA transcripts in situ. Science *280*, 585–590.

Fish, R.N., and Kane, C.M. (2002). Promoting elongation with transcript cleavage stimulatory factors. Biochim. Biophys. Acta *1577*, 287–307.

García-Martínez, J., Aranda, A., and Pérez-Ortín, J.E. (2004). Genomic run-on evaluates transcription rates for all yeast genes and identifies gene regulatory mechanisms. Mol. Cell *15*, 303–313.

García-Martínez, J., Pelechano, V., and Pérez-Ortín, J.E. (2011). Genomic methods for evaluating transcription rates in yeast. In Yeast Genetic Networks, A. Becskei, ed. (Totowa, NJ: Humana Press), pp. 25–44.

Garneau, N.L., Wilusz, J., and Wilusz, C.J. (2007). The highways and byways of mRNA decay. Nat. Rev. Mol. Cell Biol. *8*, 113–126.

Geisler, S., Lojek, L., Khalil, A.M., Baker, K.E., and Coller, J. (2012). Decapping of long noncoding RNAs regulates inducible genes. Mol. Cell *45*, 279–291.

Goler-Baron, V., Selitrennik, M., Barkai, O., Haimovich, G., Lotan, R., and Choder, M. (2008). Transcription in the nucleus and mRNA decay in the cytoplasm are coupled processes. Genes Dev. *22*, 2022–2027.

Gómez-Herreros, F., de Miguel-Jiménez, L., Morillo-Huesca, M., Delgado-Ramos, L., Muñoz-Centeno, M.C., and Chávez, S. (2012). TFIIS is required for the balanced expression of the genes encoding ribosomal components under transcriptional stress. Nucleic Acids Res. *40*, 6508–6519.

Haimovich, G., Choder, M., Singer, R.H., and Trcek, T. (2013). The fate of the messenger is pre-determined: A new model for regulation of gene expression. Biochim. Biophys. Acta. Published online January 19, 2013. http://dx.doi.org/10.1016/j.bbagrm.2013.01.004.

Harel-Sharvit, L., Eldad, N., Haimovich, G., Barkai, O., Duek, L., and Choder, M. (2010). RNA polymerase II subunits link transcription and mRNA decay to translation. Cell *143*, 552–563.

Hartzog, G.A., Wada, T., Handa, H., and Winston, F. (1998). Evidence that Spt4, Spt5, and Spt6 control transcription elongation by RNA polymerase II in Saccharomyces cerevisiae. Genes Dev. *12*, 357–369.

He, F., Li, X., Spatrick, P., Casillo, R., Dong, S., and Jacobson, A. (2003). Genome-wide analysis of mRNAs regulated by the nonsense-mediated and 5′ to 3′ mRNA decay pathways in yeast. Mol. Cell *12*, 1439–1452.

Jinek, M., Coyle, S.M., and Doudna, J.A. (2011). Coupled 5′ nucleotide recognition and processivity in Xrn1-mediated mRNA decay. Mol. Cell *41*, 600–608.

Komili, S., and Silver, P.A. (2008). Coupling and coordination in gene expression processes: a systems biology view. Nat. Rev. Genet. *9*, 38–48.

Kornberg, R.D. (2007). The molecular basis of eukaryotic transcription. Proc. Natl. Acad. Sci. USA *104*, 12955–12961.

Kruk, J.A., Dutta, A., Fu, J., Gilmour, D.S., and Reese, J.C. (2011). The multifunctional Ccr4-Not complex directly promotes transcription elongation. Genes Dev. *25*, 581–593.

Levsky, J.M., Shenoy, S.M., Pezo, R.C., and Singer, R.H. (2002). Single-cell gene expression profiling. Science *297*, 836–840.

Lohr, D., Venkov, P., and Zlatanova, J. (1995). Transcriptional regulation in the yeast GAL gene family: a complex genetic network. FASEB J. *9*, 777–787.

Lotan, R., Bar-On, V.G., Harel-Sharvit, L., Duek, L., Melamed, D., and Choder, M. (2005). The RNA polymerase II subunit Rpb4p mediates decay of a specific class of mRNAs. Genes Dev. *19*, 3004–3016.

Malagon, F., Kireeva, M.L., Shafer, B.K., Lubkowska, L., Kashlev, M., and Strathern, J.N. (2006). Mutations in the Saccharomyces cerevisiae RPB1 gene conferring hypersensitivity to 6-azauracil. Genetics *172*, 2201–2209.

Mason, P.B., and Struhl, K. (2005). Distinction and relationship between elongation rate and processivity of RNA polymerase II in vivo. Mol. Cell *17*, 831–840.

Meinhart, A., Kamenski, T., Hoeppner, S., Baumli, S., and Cramer, P. (2005). A structural perspective of CTD function. Genes Dev. *19*, 1401–1415.

Morillo-Huesca, M., Vanti, M., and Chávez, S. (2006). A simple in vivo assay for measuring the efficiency of gene length-dependent processes in yeast mRNA biogenesis. FEBS J. *273*, 756–769.

Muhlrad, D., and Parker, R. (1999). Recognition of yeast mRNAs as "nonsense containing" leads to both inhibition of mRNA translation and mRNA degradation: implications for the control of mRNA decapping. Mol. Biol. Cell *10*, 3971–3978.

Muhlrad, D., and Parker, R. (2005). The yeast EDC1 mRNA undergoes deadenylation-independent decapping stimulated by Not2p, Not4p, and Not5p. EMBO J. *24*, 1033–1045.

Page, A.M., Davis, K., Molineux, C., Kolodner, R.D., and Johnson, A.W. (1998). Mutational analysis of exoribonuclease I from Saccharomyces cerevisiae. Nucleic Acids Res. *26*, 3707–3716.

Parker, R. (2012). RNA degradation in Saccharomyces cerevisae. Genetics *191*, 671–702.

Pelechano, V., and Pérez-Ortín, J.E. (2008). The transcriptional inhibitor thiolutin blocks mRNA degradation in yeast. Yeast *25*, 85–92.

Pelechano, V., and Pérez-Ortín, J.E. (2010). There is a steady-state transcriptome in exponentially growing yeast cells. Yeast *27*, 413–422.

Pelechano, V., Jimeno-González, S., Rodríguez-Gil, A., García-Martínez, J., Pérez-Ortín, J.E., and Chávez, S. (2009). Regulon-specific control of transcription elongation across the yeast genome. PLoS Genet. *5*, e1000614.

Pérez-Ortín, J.E., Alepuz, P., Chávez, S., and Choder, M. (2013). Eukaryotic mRNA Decay: Methodologies, Pathways, and Links to Other Stages of Gene Expression. J. Mol. Biol. Published online March 4, 2013. http://dx.doi.org/10.1016/j.jmb.2013.02.029.

Pérez-Ortín, J.E., de Miguel-Jiménez, L., and Chávez, S. (2012). Genome-wide studies of mRNA synthesis and degradation in eukaryotes. Biochim. Biophys. Acta *1819*, 604–615.

Rhee, H.S., and Pugh, B.F. (2012). Genome-wide structure and organization of eukaryotic pre-initiation complexes. Nature *483*, 295–301.

Rodríguez-Gil, A., García-Martínez, J., Pelechano, V., Muñoz-Centeno, Mde.L., Geli, V., Pérez-Ortín, J.E., and Chávez, S. (2010). The distribution of active RNA polymerase II along the transcribed region is gene-specific and controlled by elongation factors. Nucleic Acids Res. *38*, 4651–4664.

Schwabish, M.A., and Struhl, K. (2007). The Swi/Snf complex is important for histone eviction during transcriptional activation and RNA polymerase II elongation in vivo. Mol. Cell. Biol. *27*, 6987–6995.

Shalem, O., Dahan, O., Levo, M., Martinez, M.R., Furman, I., Segal, E., and Pilpel, Y. (2008). Transient transcriptional responses to stress are generated by opposing effects of mRNA production and degradation. Mol. Syst. Biol. *4*, 223.

Shalem, O., Groisman, B., Choder, M., Dahan, O., and Pilpel, Y. (2011). Transcriptome kinetics is governed by a genome-wide coupling of mRNA production and degradation: a role for RNA Pol II. PLoS Genet. *7*, e1002273.

Solinger, J.A., Pascolini, D., and Heyer, W.D. (1999). Active-site mutations in the Xrn1p exoribonuclease of Saccharomyces cerevisiae reveal a specific role in meiosis. Mol. Cell. Biol. *19*, 5930–5942.

Teixeira, D., and Parker, R. (2007). Analysis of P-body assembly in Saccharomyces cerevisiae. Mol. Biol. Cell *18*, 2274–2287.

Thompson, N.L., Lieto, A.M., and Allen, N.W. (2002). Recent advances in fluorescence correlation spectroscopy. Curr. Opin. Struct. Biol. *12*, 634–641.

Titz, B., Thomas, S., Rajagopala, S.V., Chiba, T., Ito, T., and Uetz, P. (2006). Transcriptional activators in yeast. Nucleic Acids Res. *34*, 955–967.

Trcek, T., Larson, D.R., Moldón, A., Query, C.C., and Singer, R.H. (2011). Single-molecule mRNA decay measurements reveal promoter- regulated mRNA stability in yeast. Cell *147*, 1484–1497.

van Dijk, E.L., Chen, C.L., d'Aubenton-Carafa, Y., Gourvennec, S., Kwapisz, M., Roche, V., Bertrand, C., Silvain, M., Legoix-Né, P., Loeillet, S., et al. (2011). XUTs are a class of Xrn1-sensitive antisense regulatory non-coding RNA in yeast. Nature *475*, 114–117.

Zenklusen, D., Larson, D.R., and Singer, R.H. (2008). Single-RNA counting reveals alternative modes of gene expression in yeast. Nat. Struct. Mol. Biol. *15*, 1263–1271.